

Effect of Arm Dewatering using End-effector based Robotic Devices on Muscle Activity

Justin Fong¹, Vincent Crocher¹, Raneem Haddara¹,
David Ackland¹, Mary Galea², Ying Tan¹ and Denny Oetomo¹

Abstract—Dewatering of the limb is commonly performed for patients with a neurological injury, such as stroke, as it allows these patients with limited muscle activity to perform movements. Dewatering has been implemented in exoskeletons and other multi-contact devices, but not on an end-effector based device with single contact point between the assisting robot and the human limb being assisted. This study investigates the effects of dewatering using an end-effector based device on healthy subjects. The muscle activity of five subjects was measured in both static postures and dynamic movements. The results indicate a decrease in the activity of muscles which typically act against gravity — such as the anterior deltoid and the biceps brachii — but also suggest an increase in activity in muscles which act with gravity — such as the posterior deltoid and the lateral triceps. This can be explained by both the change in required muscle-generated torques and a conscious change in approach by the participants. These observations have implications for neurorehabilitation, particularly with respect to the muscle activation patterns which are trained through rehabilitation exercises.

Keywords—Dewatering, neurorehabilitation, robotics, upper limb

I. INTRODUCTION

Each year, more than 15 million people experience their first stroke, with approximately two in three surviving. Unfortunately a large proportion of stroke survivors remain disabled after their incident, with up to two in three being permanently disabled [1]. Providing adequate opportunities for rehabilitative exercise to these survivors remains a challenge for health systems around the world.

Robotic devices have been viewed as tools which can be used to improve accessibility to upper limb training after stroke [2], given their ability to mechanically assist movements. Such devices are commonly developed for those with muscle weakness, which limits their capacity to exercise independently. These devices take the form of either an exoskeleton, which aims to provide a robotic joint for each controlled physiological joint (such as the ARMin [3]), or end-effector based devices, which make contact with the arm at only a single location (such as the ADLER [4] or the EMU [5]).

A common practice in rehabilitation for people with muscle weakness in the upper limb is the mechanical dewatering of the arm through providing external support.

This allows the patients to use their limited muscle function to initiate movements, without first having to overcome the effects of gravity [6]–[8]. Control strategies for achieving this have been developed for both exoskeleton-style robotic devices [9], and recently, in a previous work by the authors, for end-effector based devices [10].

Although the goal of dewatering the arm is to reduce the muscle activation levels required to hold or move the patient’s arm, the support itself is provided only at the joint movement level (as opposed to directly assisting individual muscles). Dewatering therefore does not uniformly decrease the activation levels across all muscles or even muscle groups for a given movement. As neurorehabilitation often focuses on retraining muscle recruitment and muscle activation patterns, it is important that when analysing a robotic control strategy, the effects at the muscle level are considered.

Therefore, the goal of this work was to evaluate the effect of a dewatering control algorithm on muscle recruitment. Previous analyses have been conducted for the exoskeleton devices [9], [11], as well as passive dewatering devices [12], [13] but is yet to be applied to the end-effector based robotic concept. The use of an end-effector based device means that the effects of gravity in the joint space cannot be completely compensated for, as the device provides support at a single point of the human arm. The work sought to understand the consequences of such conditions through the use of an experimental protocol investigating both static postures and dynamic movements.

II. DEWEIGHTING ALGORITHM

The dewatering algorithm evaluated within this work was introduced and validated using a mechanical arm in [10]. However, a brief overview is provided here.

The algorithm is derived by modelling the human arm as a two-link mechanism with 3 intersecting revolute joints representing the shoulder (S) and a single revolute joint representing the elbow (E) (see Figure 1). It is assumed that the robotic device is capable of applying a generalised force ($\mathbf{f}_r, \mathbf{m}_r$) at its end-effector to the human wrist (W).

The equation of motion of the human arm, which can be written in the following form, is then considered:

$$M_h(\mathbf{q}_h)\ddot{\mathbf{q}}_h + C_h(\mathbf{q}_h, \dot{\mathbf{q}}_h)\dot{\mathbf{q}}_h + \mathbf{g}_h(\mathbf{q}_h) = \boldsymbol{\tau}_h, \quad (1)$$

where $M_h(\mathbf{q}_h) \in \mathbb{R}^{4 \times 4}$, $C_h(\mathbf{q}_h, \dot{\mathbf{q}}_h) \in \mathbb{R}^{4 \times 4}$ and $\mathbf{g}_h(\mathbf{q}_h) \in \mathbb{R}^4$ are the mass, Coriolis matrix and gravity components of

¹Melbourne School of Engineering, the University of Melbourne

²Faculty of Medicine, Dentistry and Health Sciences, the University of Melbourne

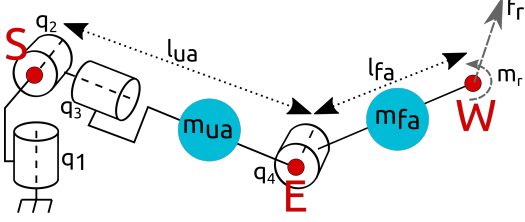


Fig. 1: The two-link mechanism representing the arm. q_{1-3} combine to represent the shoulder joint, and q_4 represents the elbow joint. $l_{ua}, l_{fa}, m_{ua}, m_{fa}$ represent the lengths and masses of the upper and forearms respectively.

the human arm, and $\tau_h \in \mathbb{R}^4$ is the torque at each joint generated by the human through their muscles.

The objective of the dewatering algorithm is for the robot to apply a generalised force ($\mathbf{f}_r, \mathbf{m}_r$) to compensate for the $\mathbf{g}_h(\mathbf{q}_h)$ component of the equation of motion of the human arm, such that τ_h , the force required to be produced by the human muscles, is reduced. This can be calculated using information about the posture of the arm (\mathbf{q}_h).

The robotic device (EMU, [5]) utilised in this experiment is underactuated, with only 3 actuated degrees of freedom, applying \mathbf{f}_r but no moment ($\mathbf{m}_r = 0$) through its end-effector to the human wrist. The force applied at the end-effector is therefore of the form:

$$\mathbf{f}_r = J_h^{T\#}(\mathbf{q}_h)\mathbf{g}(\mathbf{q}_h), \quad (2)$$

where $J_h^{T\#}(\mathbf{q}_h)$ is the posture-dependent generalised inverse of the Jacobian of the human's arm.

III. METHODS

This study investigated the effects of the dewatering algorithm on human subjects, through the implementation on the EMU upper limb rehabilitation robotic device and the measurement of electromyographic (EMG) data in static and dynamic conditions. Five healthy male subjects (age 27.4 ± 4.7 years, weight 62.6 ± 9.1 kg) were included in this study, which was approved by The University of Melbourne Human Ethics Advisory Group (ID: 1749444).

A. Apparatus and Parameters

The proposed method requires an estimation of anthropomorphic parameters of the subject — namely the masses (m_{ua} and m_{fa}), lengths (l_{ua} and l_{fa}) and locations of the centres of mass (l_{cua} and l_{cfa}) of the upper-arm and forearm. Lengths were directly measured prior to the experiment and segment masses were estimated based on the body mass of each subject according to Harless' ratios reported in [14].

The EMG data of 6 muscles used in activities of daily living: the biceps brachii (BB), lateral triceps (LT), posterior deltoid (PD), anterior deltoid (AD), pectoralis major (PM) and upper trapezius (UT) were recorded simultaneously by pre-amplified EMG surface electrodes (Cometa, Bareggio,

Italy) at 2000Hz. All electrodes were placed in correspondence to [15] except for the PM which was placed centrally in the sternocostalis area [16].

The posture of the subjects was measured using TrakStar magnetic sensors (Ascension Technologies, USA), which were used to measure the orientations of the upper arm and forearm. It was assumed that the subject remained seated upright throughout the experiment.

B. Protocol

The protocol investigated both static and dynamic conditions. At the start of each session, the EMG sensors were placed on the 6 areas of interest. The Maximum Voluntary Contraction (MVC) of each muscle was measured. Following this, the subject was seated, attached to the EMU robot and magnetic sensors used to measure the subject's posture were attached. Data were captured for the static and dynamic conditions as follows:

1) *Static Condition:* The static condition tested the ability of the device to reduce muscle activity when a subject's arm was not moving. Four postures were tested, as detailed in Table I, and visualised in Figure 2. Postures 1 to 3 were chosen as they demonstrate progressively increasing amount of joint torques to compensate for the gravity of the arm — through progressive increases of both the shoulder elevation and elbow extension — whilst remaining functional postures. Posture 4 was chosen explicitly to investigate the effects of the unactuated wrist joint of the EMU robot [10] — that is the robot cannot produce a torque around the swivel angle [17].

TABLE I: Static Postures

Posture	q_1	q_2	q_3	q_4
P1	10	20	0	10
P2	10	40	0	90
P3	10	80	0	30
P4	25	80	75	45

*Angles are reported in degrees, with reference to Figure 1

For each posture, the subject's arm was positioned based on the measurement feedback given on a computer monitor, as measured by the magnetic sensors. The subject was considered 'in posture' if the angle error of each joint was less than 5° .

Once the subject was at the desired posture, the robotic device was set one of two modes — the Transparent mode, where no force was applied onto the human subject's arm and the Dewatering mode, with the dewatering algorithm activated. In each mode, the subject was asked to maintain that posture and the EMG data were measured for 10 seconds, although the subject was not made aware of the start of the recording until the data capture had finished.

2) *Dynamic Condition:* Two movements were studied. The first movement — the "reaching movement" originated with the hand at the subject's upper thigh in a seated position, with a physical target placed at 80% of the subject's maximum reach, directly forward, and at shoulder height.



Fig. 2: The four postures used in the Static Condition tests.

The second movement — the “nose touch movement” — originated with the hand at the subject’s knee, and ended at the subject’s nose. These movements were chosen due to their functional relevance.

A metronome was set to one beat every 1.5 seconds, and the subjects were asked to move back and forward along the movement path every 1.5 seconds (*i.e.* 1.5 seconds from initial to final position and 1.5 seconds to return to the initial position). This was repeated for both “transparent” and “deweighted” robot conditions, with EMG data captured for 3 complete cycles — once again, the subjects were not advised of when this recording had started.

C. Analysis

The EMG signals of all muscles were filtered with a 2nd order Butterworth band-pass filter at 20Hz-400Hz. Following this, the static and dynamic conditions were processed through the following methods.

1) *Static Condition*: For each subject s , posture p , condition c (transparent and deweighting) and muscle group m , the Root Mean Square (RMS) value of a 3 seconds period starting at 2.5 seconds was computed ($RMS(e_{s,c,p,m})$) and normalised against the subject-specific MVC ($RMS(MVC_{s,m})$) as follows:

$$static_{s,c,p,m} = \frac{RMS(e_{s,c,p,m})}{RMS(MVC_{s,m})}. \quad (3)$$

2) *Dynamic Condition*: The captured data for each movement was segmented by manually identifying the time at which the subject first started moving (based on the location of the wrist as recorded by the robotic device). The following 1.5 seconds was taken as the forward motion, and the subsequent 1.5 seconds as the backwards motion.

The analysis was conducted in a similar way to the static condition — a normalised RMS value over the duration of the movement o . For this analysis, the forward and return directions (d) were analysed separately:

$$dyn_{s,c,o,d,m} = \frac{RMS(e_{s,c,o,d,m})}{RMS(MVC_{s,m})}. \quad (4)$$

IV. RESULTS

It is noted that due to the limited number of subjects (five), no results were statistically significant according to

the Paired Wilcoxon Signed-Rank Test ($p < 0.05$). As such, the results are presented and discussed as trends.

A. Static Condition

The percentage of MVC for each posture and each condition ($static_{s,c,p,m}$), for all subjects, are presented in Figure 3. It can be observed that in all postures in the

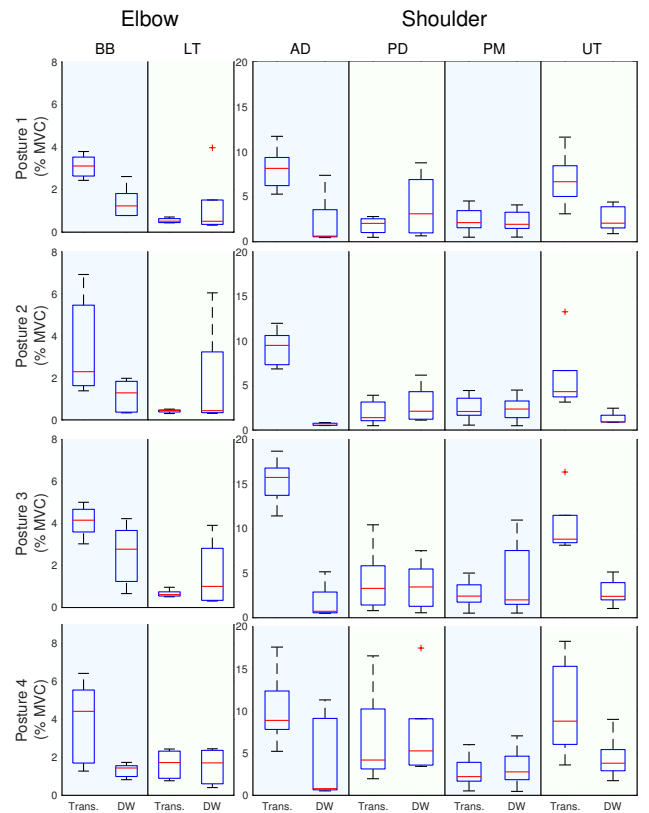


Fig. 3: Static Condition Results: Normalised RMS EMG in each posture, for biceps brachii (BB), lateral triceps (LT), posterior deltoid (PD), anteriordeltoid (AD), pectoralis major (PM), and upper trapezius (UT), under Transparent and Deweighting conditions for all subjects.

transparent condition, the AD had the largest %MVC value, indicating the importance of this muscle in sustaining the arm against gravity. It is also noted that the utilisation of

this muscle is decreased in all postures by the deweighting. This was also the case for the UT, to a smaller extent.

The muscles most significantly contributing to the control of the elbow — BB and LT — both demonstrated only a small percentage of utilisation in all postures and the data indicated that activation of the biceps decreased in all postures.

B. Dynamic Condition

The normalised overall muscle recruitment can be seen in Figure 4. Movements against gravity saw a large decrease in the recruitment of muscles, which operate against gravity in these movements — particularly when the motions were also against gravity. However, it is also noted that some muscles which operate in the same direction as gravity — LT and PD — also increased their activations in these movements.

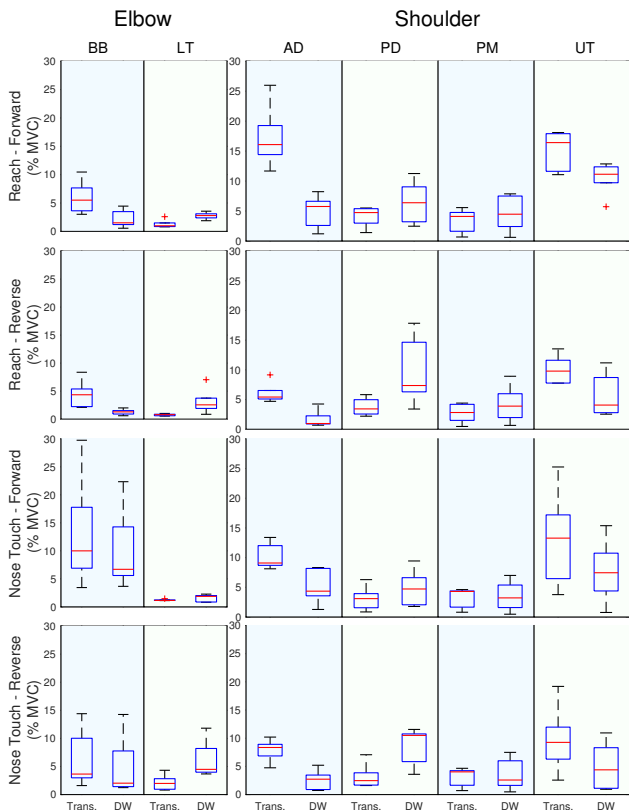


Fig. 4: Dynamic Condition Results: Normalised RMS EMG for for all subjects for biceps brachii (BB), lateral triceps (LT), posterior deltoid (PD), anterior deltoid (AD), pectoralis major (PM), and upper trapezius (UT), for each movement and direction, under Transparent and Deweighting conditions

V. DISCUSSION

A. Deweighting with End-Effector Based Devices

The results suggest that end-effector based devices are capable of compensating for the effects of gravity at both

the elbow and the shoulder — as demonstrated by the reduction in muscle activity in muscles normally recruited to compensate for the effects of gravity (the biceps brachii, upper trapezius, and anterior deltoid). This indicates that end-effector based devices are capable of providing some deweighting of the arm, and is of interest particularly when comparing such devices with exoskeletons and multi-contact sling based devices — which by construction are capable of providing this support.

B. Muscle Recruitment Changes

It is also important to note that for both the static and dynamic conditions, muscle activation change is not uniform over all muscles. In particular, although activations of the biceps brachii, anterior deltoid and upper trapezius are decreased across postures and movements, activations of the other muscles are maintained, or even increased in some postures and movements. Most notably activations of the lateral triceps and posterior deltoid were increased in almost all postures and movements. This indicates muscle co-contraction, which leads to increased subject joint impedance [18], possibly due to a reaction of the subject to the unfamiliar environment. Moreover this increase is more pronounced in movements in the direction of gravity (i.e. down). This can be explained by the fact that subjects have to counteract the gravity support provided, which does not exist in transparent — and everyday — conditions. This suggests that, in order to provide a deweighting suitable for movements in and against gravity, specific compensation strategies, relative to movement direction should be designed.

C. Implications for Neurorehabilitation

Deweighting is a commonly-employed technique for neurorehabilitation, and typically allows a patient to engage their limited muscle activity in movement of their limb. However, it is important to consider the overall objective of neurorehabilitation — to reconstruct the neuromotor loop to enable patients to use their limbs in everyday life, that is, without the assistance of machine or therapist.

This study suggests that, with an end-effector based device — but also more generally with rehabilitation robots and even therapist-supported deweighting — muscle recruitment may change besides a simple reduction. As such, possible negative effects of these changes must be balanced with the obvious benefits of providing deweighting. These effects should also be further investigated with neurologically disabled subjects who present different muscle recruitment patterns.

VI. CONCLUSION

This study investigated the effects of a deweighting strategy for a 3D end-effector based rehabilitation device for the upper limb on muscle recruitment in both static and dynamic conditions. The results indicate a decrease in the muscle activity for muscles which typically act against gravity at both elbow and shoulder, but also suggest that there is an increased activity of the antagonist muscles. This

can be explained both by the adaptation to an unfamiliar environment by the subject as well as by the deweighting strategy, making movements in the same direction as gravity more difficult. Thus, care should be taken in the use of robotic devices and deweighting in neurorehabilitation and further experiments conducted, to ensure that such differences are in the interests of the patients' recovery.

ACKNOWLEDGMENT

This work is supported by the ARC Discovery Project DP160104018.

REFERENCES

- [1] Deloitte Access Economics. The economic impact of stroke in Australia. *Melbourne: NSF*, 2013.
- [2] J Mehrholz, A Hädrich, T Platz, J Kugler, and M Pohl. Electromechanical and robot-assisted arm training for improving generic activities of daily living, arm function, and arm muscle strength after stroke. *Cochrane Database Syst Rev*, 6(6), 2012.
- [3] T Nef, M Mihelj, G Colombo, and R Riener. ARMin-robot for rehabilitation of the upper extremities. In *Proceedings 2006 IEEE International Conference on Robotics and Automation (ICRA 2006)*, pages 3152–3157. IEEE, 2006.
- [4] MJ Johnson, KJ Wisneski, J Anderson, D Nathan, and RO Smith. Development of ADLER: the activities of daily living exercise robot. In *IEEE/RAS-EMBS Int'l Conf Biomed Rob & Biomechatr (BioRob 2006)*, pages 881–886, 2006.
- [5] J Fong, V Crocher, Y Tan, D Oetomo, and I Mareels. EMU: a transparent 3D robotic manipulandum for upper-limb rehabilitation. In *IEEE International Conference on Rehabilitation Robotics (ICORR)*, pages 771–776. IEEE, 2017.
- [6] M Bartolo, AM De Nunzio, F Sebastiano, F Spicciato, P Tortola, J Nilsson, and F Pierelli. Arm weight support training improves functional motor outcome and movement smoothness after stroke. *Functional Neurology*, 29(1):15, 2014.
- [7] RF Beer, MD Ellis, BG Holubar, and J Dewald. Impact of gravity loading on post-stroke reaching and its relationship to weakness. *Muscle & Nerve*, 36(2):242–250, 2007.
- [8] R Haddara, Y Zhou, S Chinchalkar, and AL Trejos. Postoperative healing patterns in elbow using electromyography: Towards the development of a wearable mechatronic elbow brace. In *Rehabilitation Robotics (ICORR), 2017 International Conference on*, pages 1395–1400. IEEE, 2017.
- [9] F Just, Ö Özen, S Tortora, R Riener, and G Rauter. Feedforward model based arm weight compensation with the rehabilitation robot armin. In *International Conference on Rehabilitation Robotics (ICORR)*, pages 72–77. IEEE, 2017.
- [10] V Crocher, J Fong, TJ Bosch, Y Tan, I Mareels, and D Oetomo. Upper limb deweighting using underactuated end-effector based backdrivable manipulanda. *Robotics and Automation Letters*, 3(2):2116–2122, 2018.
- [11] W Wu, P Lee, J Fong, V Crocher, D Oetomo, Y Tan, and D Ackland. Modulation of shoulder muscle and joint function using a powered upper-limb exoskeleton. *J. Biomechanics*, 72:7–16, 2018.
- [12] M Coscia, V Cheung, P Tropea, A Koenig, V Monaco, C Bennis, S Micera, and P Bonato. The effect of arm weight support on upper limb muscle synergies during reaching movements. *J. Neuroengineering and Rehabilitation*, 11(1):22, 2014.
- [13] GB Prange, LAC Kallenberg, MJA Jannink, AHA Stienen, H van der Kooij, MJ IJzerman, and HJ Hermens. Influence of gravity compensation on muscle activity during reach and retrieval in healthy elderly. *J. Electromyography and Kinesiology*, 19(2):e40–e49, 2009.
- [14] R Drillis, R Contini, and M Bluestein. *Body segment parameters*. New York University, School of Engineering and Science, 1969.
- [15] HJ Hermens, B Freriks, R Merletti, D Stegeman, J Blok, G Rau, C Disselhorst-Klug, and G Hägg. European recommendations for surface electromyography. *Roessingh Research and Development*, 8(2):13–54, 1999.
- [16] H Król, G Sobota, and A Nawrat. Effect of electrode position on emg recording in pectoralis major. *J. Human Kinetics*, 17:105, 2007.
- [17] H Kim, LM Miller, A Al-Refai, M Brand, and J Rosen. Redundancy resolution of a human arm for controlling a seven DOF wearable robotic system. In *2011 Annual International Conference of the IEEE Engineering in Medicine and Biology Society*, pages 3471–3474, August 2011.
- [18] N Hogan. Impedance control: An approach to manipulation: Part II—implementation. *J. Dynamic Systems, Measurement, and Control*, 107(1):8–16, 1985.